



Research papers

Hydrologic model calibration using remotely sensed soil moisture and discharge measurements: The impact on predictions at gauged and ungauged locations



Yuan Li*, Stefania Grimaldi, Valentijn R.N. Pauwels, Jeffrey P. Walker

Department of Civil Engineering, Monash University, Clayton, Victoria 3800, Australia

ARTICLE INFO

Article history:

Received 1 June 2017

Received in revised form 26 September 2017

Accepted 6 January 2018

Available online 9 January 2018

This manuscript was handled by Marco Borga, Editor-in-Chief, with the assistance of Sankar Arumugam, Associate Editor

Keywords:

Calibration

Soil moisture

Streamflow forecasting

Remote sensing

ABSTRACT

The skill of hydrologic models, such as those used in operational flood prediction, is currently restricted by the availability of flow gauges and by the quality of the streamflow data used for calibration. The increased availability of remote sensing products provides the opportunity to further improve the model forecasting skill. A joint calibration scheme using streamflow measurements and remote sensing derived soil moisture values was examined and compared with a streamflow only calibration scheme. The efficacy of the two calibration schemes was tested in three modelling setups: 1) a lumped model; 2) a semi-distributed model with only the outlet gauge available for calibration; and 3) a semi-distributed model with multiple gauges available for calibration. The joint calibration scheme was found to slightly degrade the streamflow prediction at gauged sites during the calibration period compared with streamflow only calibration, but improvement was found at the same gauged sites during the independent validation period. A more consistent and statistically significant improvement was achieved at gauged sites not used in the calibration, due to the spatial information introduced by the remotely sensed soil moisture data. It was also found that the impact of using soil moisture for calibration tended to be stronger at the upstream and tributary sub-catchments than at the downstream sub-catchments.

© 2018 Elsevier B.V. All rights reserved.

1. Introduction

River flooding is one the most destructive natural hazards, accounting for a significant proportion of disaster-related fatalities, economic losses, and ecological damage (Pagano et al., 2014; Haynes et al., 2016). A timely, accurate, and reliable flood warning, typically achieved through an event-based or continuous streamflow forecasting system, is critical for inundation analysis, emergency preparedness and response (Sene, 2008).

As a core component of a typical streamflow forecasting system, catchment hydrologic models simulate the runoff generation, i.e., either rainfall-runoff or snowmelt-runoff, and the flow concentration and propagation processes within a catchment and its river network. While these models can be empirical, conceptual, or process-based, implemented in a lumped or distributed manner, they all suffer from uncertainties caused by forcing data, model physics, initial condition quantification, and parameter estimation. To reduce these uncertainties, and to meet the accuracy requirement of the streamflow forecasting application, these models are

typically constrained by observed data, either through batch calibration to address systematic errors using historical observations, or data assimilation to address random errors using real-time observations (Li et al., 2016). Although various data assimilation algorithms have been proposed and implemented, batch calibration is still an important and widely used tool due to the highly conceptualized parameterizations in many streamflow forecasting models (Emerton et al., 2016; Pagano et al., 2016).

To optimize their performance, hydrologic models tend to be calibrated against all available gauged streamflow data. Nevertheless, it has been found that the models have reached their accuracy limit unless new types of observations are integrated (Loumagne et al., 2001b). Thanks to recent advances in remote sensing techniques, there is a great opportunity to introduce remotely sensed land surface state variables to further improve the model performance (Grimaldi et al., 2016; Li et al., 2016).

Soil moisture is an important variable in catchment hydrologic processes (Legates et al., 2011). It is used as an indicator of catchment wetness, which is an essential initial condition for hydrologic models – it has been generally found that a wet catchment has a higher chance to lead to a high runoff ratio, and thus more likely to lead to a high-flow event, indicating a high risk of flooding

* Corresponding author.

E-mail address: yuan.li2@monash.edu (Y. Li).

(Li et al., 2014). However, the availability of ground-based soil moisture monitoring sites is limited; furthermore, these are point measurements only representing a small spatial range (Romano, 2014). Remote sensing techniques provide a tool to obtain spatially distributed near-surface soil moisture information from space. Consequently, they have attracted increased interest by hydrologic communities (Liu et al., 2012).

Remotely sensed soil moisture has been widely integrated into soil moisture accounting or land surface models to improve near-surface and/or root-zone soil moisture simulation. Meanwhile, the hydrologic communities have also introduced remotely sensed soil moisture for streamflow prediction (Li et al., 2016). Among those soil moisture constrained streamflow prediction studies, there has been a major effort on investigating the impact of soil moisture data assimilation on forecasting/hindcasting skills (Goodrich et al., 1994; Otlé and Vidal-Madjar, 1994; Loumagne et al., 2001a,b; Pauwels et al., 2001; Quesney et al., 2001; Pauwels et al., 2002; Aubert et al., 2003; Francois et al., 2003; Jacobs et al., 2003; Crow and Ryu, 2009; Brocca et al., 2010; Chen et al., 2011; Draper et al., 2011; Brocca et al., 2012; Han et al., 2012; Matgen et al., 2012; Alvarez-Garretón et al., 2014; Chen et al., 2014; Massari et al., 2014; Ridler et al., 2014; Wanders et al., 2014a,b; Alvarez-Garretón et al., 2015; Laiolo et al., 2015; Lievens et al., 2015; Cenci et al., 2016; López López et al., 2016; Yan and Moradkhani, 2016), with much fewer studies on utilizing remotely sensed soil moisture data for batch calibration (Parajka et al., 2006; Parajka et al., 2009; Sutanudjaja et al., 2014; Silvestro et al., 2015; Kunnath-Poovakka et al., 2016; Rajib et al., 2016; Kundu et al., 2017; López López et al., 2017). In-situ soil moisture data were introduced for lumped hydrologic model calibration, showing that adding soil moisture information additional to streamflow observations can improve the robustness of the model parameter estimation, which has the potential to lead to more accurate streamflow forecasts (Zhang et al., 2015; Thorstensen et al., 2016; Shahrban, 2017). However, when remotely sensed soil moisture data were used, it was found to be hard to achieve a consistent improvement in streamflow prediction (Parajka et al., 2006, 2009). Along with the development of earth observation techniques, the temporal coverage of remotely sensed soil moisture products has been significantly improved, e.g., with satellite revisit improved from 35 days in the Synthetic Aperture Radar on European Remote Sensing satellites (SAR/ERS) to 1–3 days in the Advanced Scatterometer (ASCAT), the Soil Moisture Ocean Salinity (SMOS), and the Soil Moisture Active Passive (SMAP) missions. This provides a potential to further improve the batch calibration. Recent related studies have been focused on implementing these advanced remotely sensed soil moisture products to calibrate a water resources accounting model (Kunnath-Poovakka et al., 2016), distributed hydrologic models (Sutanudjaja et al., 2014; Silvestro et al., 2015; López López et al., 2017), and semi-distributed hydrologic models (Rajib et al., 2016; Kundu et al., 2017). Certain levels of improvement on streamflow simulations were achieved by calibrating hydrologic models against remotely sensed soil moisture data compared with uncalibrated models (Kunnath-Poovakka et al., 2016; Kundu et al., 2017; López López et al., 2017). However, streamflow estimates still tended to be better when the model was calibrated against streamflow measurements (López López et al., 2017). Therefore, as Kundu et al. (2017) pointed out at the end of their article, there is a need to test the potential of using remotely sensed soil moisture data together with streamflow measurements for batch calibration of hydrologic models. A couple of studies have investigated soil moisture–streamflow joint calibration schemes (Sutanudjaja et al., 2014; Silvestro et al., 2015; Rajib et al., 2016), and it has been found that introducing soil moisture information in addition to streamflow measurements can address the equifinal-

ity issues, and thus lead to benefits in streamflow prediction. While these findings are encouraging, there has not been a study that investigated the impact of using soil moisture–streamflow joint calibration on streamflow prediction at ungauged locations, which is a practical question faced by operational hydrologic community.

From the practical perspective, it is not always the case that a catchment has either no flow gauges or a dense gauge network. There are many catchments with a limited number of flow gauges available for model calibration (e.g., http://www.bafg.de/GRDC/EN/Home/homepage_node.html). A typical example is that only one gauge at the outlet of a catchment can be used for calibration while there is a practical demand to predict streamflow at certain internal locations. In that case the forecasting/hindcasting skill in internal sub-catchments are normally not satisfactory. Remote sensing techniques provide spatially distributed information of soil moisture. However, whether including remotely sensed soil moisture data in addition to the limited number of flow gauges for model calibration can benefit forecasting at the ungauged internal locations has not been fully addressed, which is the main research question for this study.

To test the added value of including remotely sensed soil moisture for batch calibration, a joint calibration scheme using remotely sensed soil moisture and gauged streamflow data was compared with a traditional streamflow-only calibration scheme through lumped and semi-distributed model setups. The model performance was evaluated at both “gauged” (gauges used for calibration) and “ungauged” (gauges not used for calibration) locations for the calibration period as well as for an independent validation period in a hindcasting mode, i.e., with observed forcing data.

2. Catchments and data

Two catchments in southeast Australia were used for this study (Fig. 1). The first is the Clarence River catchment upstream of Lilydale. The catchment is mainly covered by eucalyptus forest with the main stream draining from northwest to southeast with a quick flow propagation (~1 day). The second is the Condamine River catchment upstream of Chinchilla, which adjoins the Clarence. The upstream area is mainly covered by eucalyptus forest while the downstream area is mainly covered by rainfed cropping farm and pasture with the main stream draining from southeast to northwest with a slow flow propagation (4–6 days). The two catchments are geographically close to each other, but the hydrologic features are quite different. The vegetation density is relatively high in the Clarence and low in the Condamine, impacting the quality of remotely sensed soil moisture products. The relatively short flow response time in the Clarence relative to the Condamine may affect the impact of initial catchment wetness on the streamflow forecasts. These different features make the two catchments a good comparative case study.

The two catchments were delineated into sub-catchments (Fig. 1) using the Australian Hydrological Geospatial Fabric (<http://www.bom.gov.au/water/geofabric/>). Specifically, this was done in two major steps:

- choose the forecasting locations and set them to be the outlets of sub-catchments; and
- delineate the boundary of each sub-catchment by tracking the contributing area upstream through the river network.

Each forecasting location was manually chosen based on two criteria: 1) there is a flow gauge available; and 2) its related sub-catchment is large enough to cover at least one SMOS pixel, e.g., with an area of over 625 km².

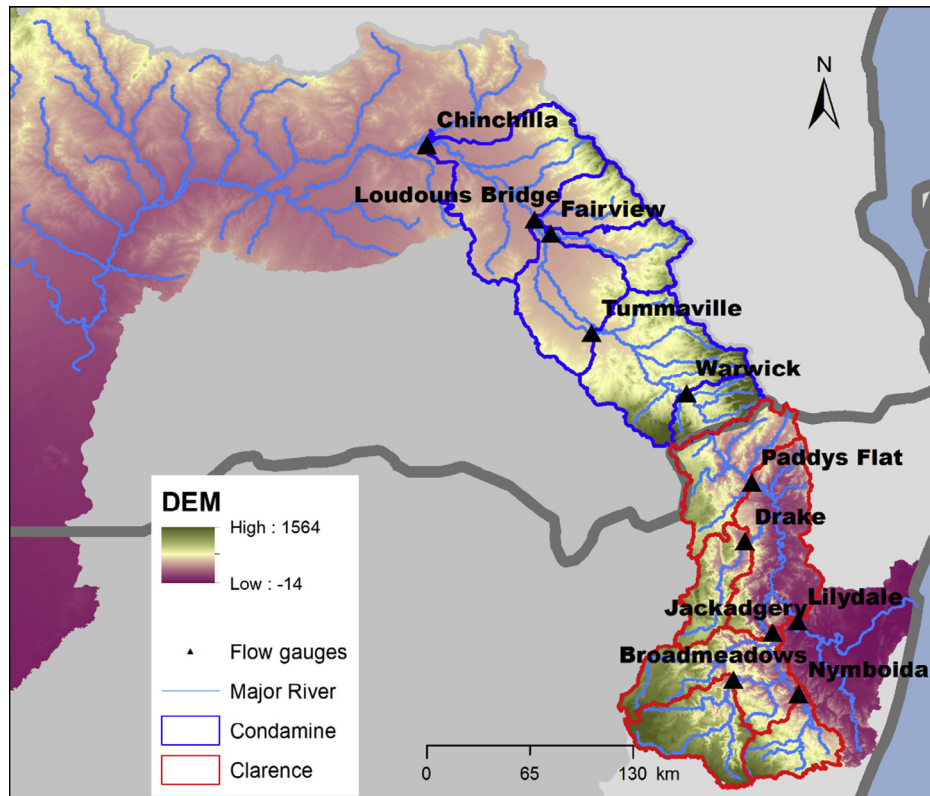


Fig. 1. Study catchments and sub-catchment delineation together with flow gauge locations.

Data used in this study include potential evapotranspiration (PET), gauged precipitation, gauged streamflow, remotely sensed near-surface soil moisture, and remotely sensed fractional vegetation cover (fc) for January 2010–June 2014. The PET, precipitation, and fc were used as model inputs, while the streamflow and soil moisture data were used for model calibration and/or validation.

The monthly gridded Australian Water Availability Project (AWAP) PET dataset (Raupach et al., 2009; Raupach et al., 2012), which was estimated from observed solar radiation using the method developed by Priestley and Taylor (1972), was used in this study. The sub-catchment PET values were extracted according to the sub-catchment boundaries (described in Section 3), and converted into hourly records with the assumption that it is constant within each month. The variability of PET within a month was ignored in this study. Nevertheless, it has been noted that the variation in PET has much less impact on streamflow than rainfall in rainfall-runoff modelling (Samain and Pauwels, 2013; Bennett et al., 2014). For this reason, the use of the monthly AWAP PET for hourly streamflow forecasting has been widely implemented in Australia (Pagano et al., 2011a; Li et al., 2014, 2015; Bennett et al., 2016).

Gauged precipitation data were quality controlled against AWAP daily rainfall based on a two-step approach (Robertson et al., 2015), including:

- inconsistent data (anomalously high or low flows) censoring based on double-mass plots; and
- low quality gauge removal according to the correlation with AWAP daily precipitation.

The quality controlled hourly rainfall was then spatially interpolated to sub-catchments from rain gauges within a 10 km range of each entire catchment using an inverse distance weighted method.

Six streamflow gauges from the Clarence and five from the Condamine were selected as calibration/validation locations (detailed in Section 3.3), according to the continuity of the streamflow data and needs for the sub-catchment delineation. Hourly streamflow data of the Clarence and Condamine basins were obtained from the New South Wales Department of Primary Industries Water (<http://www.water.nsw.gov.au/>) and the Queensland Department of Natural Resources and Mines (<https://water-monitoring.information.qld.gov.au/>), respectively.

Soil moisture was extracted from the SMOS level 3 product (reanalysis version) provided by the “Centre Aval de Traitement des Données SMOS” (CATDS), which is a grid-based dataset with an ascending pass at about 6 am and a descending pass at about 6 pm (local time). The approximate 43 km resolution data have been posted onto a grid size of about 25 km with a temporal revisit of 1–3 days. The soil moisture data were extracted according to the sub-catchment boundaries and then averaged into each sub-catchment by area weighting average.

The monthly fc was retrieved from the Moderate Resolution Imaging Spectroradiometer (MODIS) data by the Commonwealth Scientific and Industrial Research Organisation (CSIRO) with a resolution of 500 m. As the scale of the fc data is much smaller than the scale of the sub-catchments, the fc data were extracted by the sub-catchment boundaries and then directly averaged for each sub-catchment. The fc was also assumed to be constant within each month.

3. Methodology

3.1. Experiment design

Riverine flood forecasting can be performed using a lumped or distributed/semi-distributed catchment modelling system,

depending on the catchment size, availability of streamflow gauges, and rain gauge density. In this study, two calibration schemes were applied in three model setups for a total of six experiment scenarios (Table 1). The two calibration schemes were 1) a traditional calibration using gauged streamflow only; and 2) a joint calibration using both streamflow and soil moisture data. The three model setups were 1) a lumped model; 2) a semi-distributed model (Semi-1) with the assumption that only one streamflow gauge at each catchment outlet was available for model calibration; and 3) a semi-distributed model (Semi-2) with the assumption that all the streamflow gauges at the outlets of the sub-catchments were available for calibration.

The catchment/sub-catchment boundaries are shown in Fig. 1. The PET, f_c , and soil moisture were sampled into either a single value for each catchment (for the lumped model) or different values for the sub-catchments (for the Semi-1 and Semi-2). The precipitation was interpolated into the centroids of the sub-catchments for Semi-1 and Semi-2, and then integrated into a single value for the lumped model by area-weighted average according to the areas of the sub-catchments. For the Semi-1, the same set of parameters was estimated for all sub-catchments, while all other internal sub-catchments were assumed to be “ungauged” and the measurements there were only used for validation. For the Semi-2, each sub-catchment was calibrated in sequence from upstream to downstream using the gauged streamflow at its outlet. The streamflow and soil moisture data used for calibration were assumed to be accurate, i.e., observational uncertainties were not considered.

3.2. The hydrologic model

GR models (modèle du Génie Rural) have been widely used by operational hydrologic forecasting communities. For instance, the Australian Bureau of Meteorology incorporates the GR4H (an hourly 4 parameter GR model) as the core of their operational 7-day streamflow forecasting service (<http://www.bom.gov.au/water/7daystreamflow/>). One challenge of using remotely sensed near-surface soil moisture data to constrain the GR4H is the different meaning of soil moisture between the model and the remote sensing data. Specifically, like many other conceptual rainfall-runoff models, the GR4H parameterizes the catchment wetness into a single bulk soil water storage, which is not directly comparable with remotely sensed near-surface soil moisture. To better accept remote sensing information, Loumagne et al. (1996) reparameterized the soil water storage of the GR4J (a daily version of GR4H) into a two layer system, namely the GRHUM, in which a near-surface soil moisture layer is embedded into the bulk soil moisture layer and the two layers have the same rainfall input. Francois et al. (2003) improved the original GRHUM into a new version, namely the GRKAL, in which two independent near-surface and root-zone soil moisture layers are parameterized and

the drainage from the near-surface layer is used as the input for the root-zone layer.

In this study, an hourly version of the GRKAL was adopted to simulate the rainfall-runoff and catchment routing processes. Fig. 2 provides a schematic of the model. The model can be viewed as two sub-models: 1) a two-layer soil moisture accounting sub-model; and 2) a catchment routing sub-model. In the soil moisture accounting sub-model, the total precipitation Pn is firstly split into infiltration (Ps) and direct runoff ($Pn-Ps$). Ps entering into the near-surface soil layer is then drained through a two-layer soil system. The actual total evapotranspiration (ET) is calculated as the sum of the ET from the near-surface layer and the transpiration from the root-zone layer. The output of the near-surface layer is used as the input for the root-zone layer (hydraulic exchange), and the final output of the two-layer system is the percolation from the root-zone layer ($Perc$). The $Perc$ is then added to $Pn-Ps$ as a total runoff (Pr) which then enters the catchment routing sub-model.

The catchment routing part of the GRKAL is essentially the same as that of the GR4H, i.e., it incorporates two unit hydrographs and one nonlinear routing storage to represent the time delay caused by the runoff concentration process. Specifically, Pr is divided into two parts with a fixed ratio: 10% of Pr is routed through a single unit hydrograph (UH2) while 90% of Pr is routed through a cascade of another unit hydrograph (UH1) and a routing store (R). F nominally represents underground water exchanges between the modelled catchment and the adjacent catchments. Details about the model were described by Francois et al. (2003).

In the lumped model setup, the GRKAL was used as a standalone tool to simulate the rainfall-runoff, the overland flow routing, and the river channel routing processes. In the semi-distributed model setups (the Semi-1 and Semi-2), the GRKAL was used to simulate the hydrologic processes in each sub-catchment, and the output of the GRKAL from each sub-catchment was entered into a linear Muskingum river model and routed to the outlet of the entire

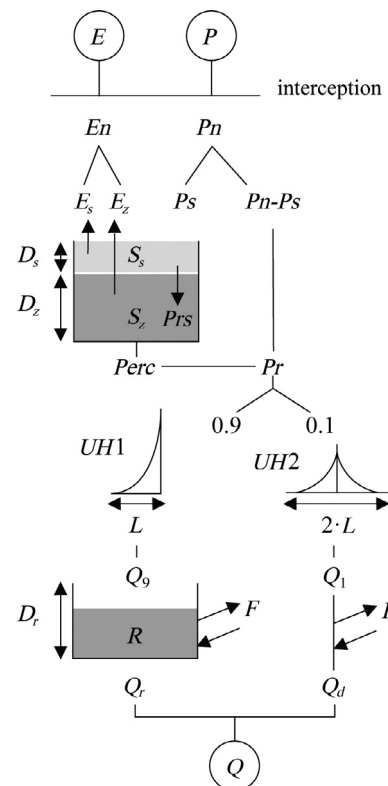


Fig. 2. The structure of the GRKAL model (Francois et al., 2003).

Table 1
Experiment scenarios tested.

Scenario alias	Model setup	Calibration scheme
Lumped Q-Cali	Lumped model	Streamflow calibration
Lumped Joint-Cali		Joint calibration
Semi-1 Q-Cali	Semi-distributed with one streamflow gauge available at the outlet	Streamflow calibration
Semi-1 Joint-Cali		Joint calibration
Semi-2 Q-Cali	Semi-distributed with multiple streamflow gauges available	Streamflow calibration
Semi-2 Joint-Cali		Joint calibration

catchment. The Muskingum model simplifies the shallow water equations based on a finite-difference approximation. It parameterizes the water storage in the flow wave and river network through a triangular wedge and rectangular prism. Details about the Muskingum model were described by Nash (1959) and Cunge (1969).

3.3. The calibration approach

The streamflow-only calibration was designed according to the strategy implemented in the operational 7-day streamflow forecasting service by Australian Bureau of Meteorology. The Shuffled Complex Evolution-University of Arizona algorithm (SCE-UA) (Duan et al., 1992), which is currently used for the 7-day streamflow forecasting, was used to find the globally optimal parameter set. For the objective function, it has been a tradition in the course of developing the forecasting system in Australia to use an unweighted average of several metrics sensitive to different range of flows, e.g., high flows, low flows, mid-range flows, and bias (Pagano et al., 2011b; Bennett et al., 2014; Li et al., 2015; Bennett et al., 2016). This is because the use of a hybrid objective can strength its ability to result in a more robust model to better simulate the whole range of flows, which is also important in the catchments investigated in this paper, e.g., drought and floods are frequent in the Condamine and can happen during the same year. Therefore, the objective function chosen in this study (Eq. (1)), is expressed as an unweighted mean of two Nash-Sutcliffe model efficiency scores of log transformed flows (sensitive to low flows, Eq. (2)) and Box-Cox transformed flows (sensitive to mid-range flows, Eq. (3)), a Kling-Gupta efficiency coefficient score (sensitive to high flows and variance, Eq. (4)), and a mean Bias score (Eq. (5)).

$$F_Q = F_{\log NS} + F_{\text{BoxNS}} + F_{KGE} + F_{\text{bias}}, \quad (1)$$

where

$$F_{\log NS} = \frac{\sum_{t=1}^{T_c} [\ln(Q_{\text{sim},t} + v) - \ln(Q_{\text{obs},t} + v)]^2}{\sum_{t=1}^{T_c} [\ln(Q_{\text{sim},t} + v) - \ln(\bar{Q}_{\text{obs},t} + v)]^2}, \quad (2)$$

$$F_{\text{BoxNS}} = \frac{\sum_{i=1}^{T_c} (Q'_{\text{sim},t} - Q'_{\text{obs},t})^2}{\sum_{i=1}^{T_c} (Q'_{\text{sim},t} - \bar{Q}'_{\text{obs}})^2}, \quad (3)$$

$$F_{KGE} = \sqrt{(1-r)^2 + \left(1 - \frac{\sigma_{\text{sim}}}{\sigma_{\text{obs}}}\right)^2 + \left(1 - \frac{\bar{Q}_{\text{sim}}}{\bar{Q}_{\text{obs}}}\right)^2}, \quad (4)$$

$$F_{\text{bias}} = \left[\max\left(\frac{\bar{Q}_{\text{sim}}}{\bar{Q}_{\text{obs}}}, \frac{\bar{Q}_{\text{obs}}}{\bar{Q}_{\text{sim}}}\right) - 1 \right]^2, \quad (5)$$

with $Q_{\text{sim},t}$ and $Q_{\text{obs},t}$ being streamflow simulations and observations at time t in the calibration period T_c ; v is the smallest non-zero streamflow observation in T_c ; r is the Pearson correlation coefficient between Q_{sim} and Q_{obs} ; $Q'_{\text{sim},t}$ and $Q'_{\text{obs},t}$ are the Box-Cox transformed streamflow, which can be expressed as

$$Q' = \frac{(Q + 1)^\gamma - 1}{\gamma}, \quad (6)$$

where γ denotes a transformation parameter, which was set to be 0.3 as suggested by Li et al. (2015).

For the joint calibration scheme, a joint objective function, which is essentially a weighted average between the objective function for streamflow and the objective function for soil moisture, was proposed in this study as

$$F_{\text{joint}} = a \cdot F_Q + (1 - a) \cdot F_{SM}, \quad (7)$$

where a is a weighting coefficient and F_{SM} is a single Nash-Sutcliffe model efficiency score between the modelled ($S_{\text{sim},t}$) and remotely sensed soil moisture ($S_{\text{obs},t}$) as

$$F_{SM} = \frac{\sum_{i=1}^{T_c} (S_{\text{sim},t} - S_{\text{obs},t})^2}{\sum_{i=1}^{T_c} (S_{\text{sim},t} - \bar{S}_{\text{obs}})^2}. \quad (8)$$

A key point of the joint objective function is to define a so as to appropriately emphasize the importance of soil moisture information. In the original GRKAL paper, Francois et al. (2003) suggested to give a weight of 5/7 to streamflow, when near-surface soil moisture, root-zone soil moisture, and streamflow were jointly used for model calibration, with the justification that streamflow should account for a larger weight than soil moisture as the objective was streamflow forecasting. Nevertheless, only near-surface soil moisture data was used in this study and therefore it was not justified to adopt the weight suggested in that paper. With the consideration of their suggestion, a trial-and-error process was applied to analyze a suitable value of a . Values of 0.5, 0.6, 0.7, 0.8, and 0.9 were tested, resulting in minimum objective function values of 0.19, 0.16, 0.15, 0.18, and 0.20 in the Clarence, and 0.36, 0.31, 0.27, 0.29, and 0.33 in the Condamine respectively, for the Semi-1 model setups. Therefore, the value of 0.7 for a was chosen for this study as it exhibited the lowest objective function value.

In the lumped model setup, only one lumped model parameter set was obtained through calibration. In the Semi-1 model setup (described in Table 1), as only the gauge at the catchment outlet was assumed to be available for calibration, parameters were set to be spatially uniform for all sub-catchments to reduce potential equifinality issues due to over-parameterization, except for the parameter L (Fig. 2) representing the length of the two unit hydrographs. As shown by Li et al. (2013), the natural response time of Australian catchments can typically be formulated as a power function of the catchment area; therefore, the calibrated L was scaled by the square root of each sub-catchment area to represent the natural concentration delay. In the Semi-2 model setup, as all internal and outlet gauges were used for calibration, the calibration was done from the upstream sub-catchments to the downstream sub-catchments, and independent parameter sets were estimated for sub-catchments.

4. Results

The hourly hydrologic model was calibrated for all six scenarios specified in Table 1 using the data from January 2010 to December 2012, with the first three months being a warm-up period. The calibrated parameter sets were then applied for model prediction in an independent validation period, from January 2013 to June 2014, through a hindcasting mode. The performance of the modelling system was evaluated in both the calibration and validation periods in terms of streamflow predictions. Two statistics, including the Nash-Sutcliffe model efficiency coefficient (NS) and F_Q defined in Eq. (1), were used to evaluate the accuracy of the streamflow predictions, as shown in Tables 2–5. More specifically, Tables 2 and 3 list NS and F_Q in the Clarence catchment for the calibration and validation periods, respectively. Tables 4 and 5 show the same results for the Condamine catchment. Both statistics were calculated for the continuous hourly streamflow predictions within the whole calibration/validation period. The NS was used to evaluate the predictive skill with an emphasis on high flows, while F_Q was used to demonstrate the model performance in accordance with the objective function used for calibration. Higher NS and lower F_Q values indicate a better model prediction.

Table 2

NS/ F_Q values of streamflow prediction in the Clarence River catchment during the calibration period. Bold numbers indicate where the joint calibration (Joint-Cali) improved the streamflow prediction compared with streamflow calibration (Q-Cali), while standard font numbers indicate where Joint-Cali performed worse than or equivalent to Q-Cali. The box highlights the “ungauged” cases.

Model setup	Calibration scheme	Lilydale	Jackadgery Nymboida	Broad-meadows	Drake	Paddys Flat
Lumped	Q-Cali	0.71/0.29	-	-	-	-
	Joint-Cali	0.68/0.34	-	-	-	-
Semi-1	Q-Cali	0.83/0.14	0.65/0.39	0.58/0.45	0.43/0.55	0.45/0.55
	Joint-Cali	0.81/0.15	0.67/0.34	0.54/0.48	0.59/0.42	0.50/0.47
Semi-2	Q-Cali	0.85/0.13	0.84/0.11	0.82/0.17	0.72/0.25	0.81/0.14
	Joint-Cali	0.82/0.15	0.83/0.11	0.79/0.19	0.70/0.28	0.76/0.21

Table 3

As for Table 2 but for the validation period.

Model setup	Calibration scheme	Lilydale	Jackadgery Nymboida	Broad-meadows	Drake	Paddys Flat
Lumped	Q-Cali	0.59/0.42	-	-	-	-
	Joint-Cali	0.62/0.38	-	-	-	-
Semi-1	Q-Cali	0.74/0.29	0.61/0.41	0.57/0.45	0.48/0.49	0.42/0.60
	Joint-Cali	0.76/0.30	0.62/0.39	0.52/0.47	0.55/0.42	0.46/0.50
Semi-2	Q-Cali	0.79/0.19	0.77/0.25	0.74/0.26	0.65/0.34	0.71/0.30
	Joint-Cali	0.78/0.22	0.77/0.22	0.72/0.28	0.68/0.31	0.73/0.25

Table 4

As for Table 2 but for the Condamine catchment during the calibration period.

Model setup	Calibration scheme	Chinchilla	Loudouns Bridge	Tummaville	Warwick	Fairview
Lumped	Q-Cali	0.54/0.49	-	-	-	-
	Joint-Cali	0.48/0.55	-	-	-	-
Semi-1	Q-Cali	0.70/0.27	0.62/0.40	0.47/0.49	0.49/0.46	0.54/0.44
	Joint-Cali	0.69/0.29	0.64/0.37	0.55/0.42	0.60/0.37	0.51/0.46
Semi-2	Q-Cali	0.77/0.20	0.76/0.23	0.81/0.16	0.83/0.15	0.73/0.25
	Joint-Cali	0.74/0.22	0.73/0.28	0.73/0.25	0.79/0.19	0.69/0.29

Table 5

As for Table 2 but for the Condamine catchment during the validation period.

Model setup	Calibration scheme	Chinchilla	Loudouns Bridge	Tummaville	Warwick	Fairview
Lumped	Q-Cali	0.49/0.50	-	-	-	-
	Joint-Cali	0.48/0.52	-	-	-	-
Semi-1	Q-Cali	0.63/0.44	0.55/0.47	0.46/0.56	0.45/0.56	0.50/0.51
	Joint-Cali	0.65/0.43	0.58/0.45	0.51/0.50	0.55/0.44	0.44/0.54
Semi-2	Q-Cali	0.69/0.25	0.69/0.27	0.75/0.25	0.75/0.25	0.68/0.29
	Joint-Cali	0.70/0.23	0.71/0.23	0.72/0.27	0.76/0.23	0.67/0.28

4.1. Comparison among models

For the lumped model setup, the entire catchment (Clarence/Condamine) was assumed to be one bucket, and the streamflow was only simulated at the catchment outlet (Lilydale/Chinchilla). Therefore, the evaluation statistics (NS and F_Q) were not calculated

at the internal locations for the lumped modelling scenarios. According to Tables 2–5, the lumped model resulted in a much lower NS and higher F_Q values compared with semi-distributed models, in both catchments and both the calibration and validation periods. For instance, the Q-Cali for the lumped model gave a NS/ F_Q of 0.71/0.29 at Lilydale and 0.54/0.49 at Chinchilla during the cal-

ibration period, which were worse than the 0.83/0.14 and 0.70/0.27 obtained for the Semi-1 at Lilydale and Chinchilla respectively. This indicates that the lumped model is not suitable for such large catchments. Lumped systems are generally limited in representing the spatial distribution of forcing and parameters, which can lead to unsatisfactory results for large catchments. In the Condamine, the main river is long, the catchment shape is narrow, and the flow velocity is slow due to the relatively flat topography. Therefore, the unit hydrograph type routing in the GRKAL is not suited to simulate the flow propagation in this river system. For this reason, the performance of the lumped model at Chinchilla was even worse than that at Lilydale according to the NS and F_Q values shown in Tables 2–5.

The semi-distributed model calibrated against all internal and outlet gauges (Semi-2) generally outperformed the model calibrated against only the outlet gauge (Semi-1). The difference between the Semi-1 and Semi-2 was relatively slight at the catchment outlets, e.g., the differences in NS/ F_Q between the two systems were 0.02/0.01 at Lilydale and 0.07/0.07 at Chinchilla, respectively, during the calibration period in Q-Cali. This is because both semi-distributed models employ distributed forcing and model structures, while the only difference being that the parameters were distributed in space in the Semi-2 but set to be uniform in the Semi-1. However, the performance differences were much more obvious at internal locations. This is expected as the internal sub-catchments were not calibrated against the internal gauges in the Semi-1.

The relative strength of the three model setups did not change when soil moisture was included in the calibration, i.e., the Semi-2 still performed best (with the NS between 0.65 and 0.82, and the F_Q between 0.11 and 0.30) while the lumped was still the worst (with the NS between 0.48 and 0.68, and the F_Q between 0.29 and 0.55). However, the impact of soil moisture on streamflow prediction varied among different modelling settings. In the lumped and Semi-2 scenarios, the joint calibration scheme generally degraded the NS and F_Q during the calibration periods compared with the traditional streamflow calibration scheme (with a NS decrease between 0.01 and 0.08, and a F_Q increase between 0 and 0.07 as shown in Tables 2–5). Nevertheless, a certain level of improvement was seen in the validation period at some of the gauges. More consistent improvement by using soil moisture information was obtained in the Semi-1 in both the calibration and validation periods. It should be noted that in the Semi-1, all the internal sites were assumed to be “ ungauged”, while in the lumped and Semi-2 setups, all evaluations were conducted at “ gauged” locations.

4.2. Impact of soil moisture at gauged locations

The predictions at “ ungauged” locations are highlighted by the boxes in Tables 2–5, and thus the “ gauged” examples are those outside the boxes. The NS and F_Q values summarized in Tables 2–5 indicate a consistent degradation in streamflow caused by using soil moisture data at gauged locations during the calibration period. This is also illustrated in Fig. 3 (a and c) – during the events in the calibration period, the joint calibration led to worse predictions compared with the streamflow calibration at both Lilydale and Chinchilla. This is reasonable as minimizing error in streamflow was expected to lead to optimal streamflow estimation, while introducing additional soil moisture information sacrificed the optimality of the streamflow simulation to reduce errors in the soil moisture. Nevertheless, although the degradation was consistent in the calibration period, it is encouraging to find the forecasts were improved. This can be explained as an equifinality issue in streamflow optimization – different parameter sets can lead to

similar performance for streamflow but with different results for other variables, such as near-surface soil moisture (Sutanudjaja et al., 2014; Silvestro et al., 2015). Therefore, minimizing errors from both near-surface soil moisture and streamflow has the potential to lead to more robust parameter sets which improve the modelled soil moisture without impeding streamflow predictability significantly in the calibration period. The improved robustness then has the potential to result in more accurate streamflow future forecasts – this was to a certain extent shown in this case study. Considering all the gauges in the two catchments for the three model setups (Table 3 and 5), 9 out of 15 gauged cases were improved in terms of NS while 10 out of 15 were improved in terms of F_Q by joint calibration in the independent validation period. The events in the validation period at Lilydale and Chinchilla are shown in Fig. 3 (b and d): the improvement was observed during the first peak flow at Lilydale, while similarly during both flood peaks at Chinchilla.

4.3. Impact of soil moisture at ungauged locations

The predictions at “ ungauged” locations are highlighted by the boxes in Tables 2–5. Contrary to the “ gauged” locations, streamflow predictions at “ ungauged” locations were found to be more consistently improved by using soil moisture for the calibration. Specifically, 4 locations out of 5 in the Clarence and 3 locations out of 4 in the Condamine exhibited a higher NS and a lower F_Q by joint calibration in both the calibration and validation periods. This is also illustrated in Fig. 4, which shows that the joint calibration improved the prediction of some of the flood peaks in the calibration and validation events at Paddys Flat and Tummaville. The improvement was more obvious than in gauged locations. This can be explained as follows. When streamflow gauges are limited, the spatially distributed soil moisture information becomes the only information for internal sub-catchments. Introducing soil moisture into the model calibration essentially strengthens the model in predicting the spatial variability of hydrologic variables, e.g., soil moisture and streamflow.

5. Discussion

5.1. Impact of sub-catchment locations

The impact at the “ ungauged” sub-catchments caused by introducing soil moisture information was found to vary with the location of the sub-catchments. For instance, the difference in NS between the streamflow calibration and the joint calibration was relatively small at the downstream locations, e.g., Jackadgery in the Clarence and Loudouns Bridge in the Condamine, while the differences tended to be larger at the upstream and tributary locations, e.g., Paddys Flat, Drake, Broadmeadows, and Nymboida in the Clarence, as well as Warwick, Tummaville, and Fairview in the Condamine. A similar pattern was also found in F_Q values. This can be explained by the fact that the downstream locations are closer to the calibration gauge, and thus more constrained by the streamflow data. The upstream and tributary sub-catchments compensated each other to optimize the flow prediction at the outlet, being more sensitive to the spatial variability brought by the soil moisture information. This was extremely obvious at Warwick, whose NS/ F_Q was improved from 0.49/0.46 to 0.60/0.37 in the calibration period and 0.45/0.56 to 0.55/0.44 in the validation period, as it was the most distant sub-catchment to Chinchilla in a long river system.

It should be pointed out that not all upstream and tributary sub-catchments were improved by using soil moisture, e.g., degradations were found at Nymboida and Fairview in both the

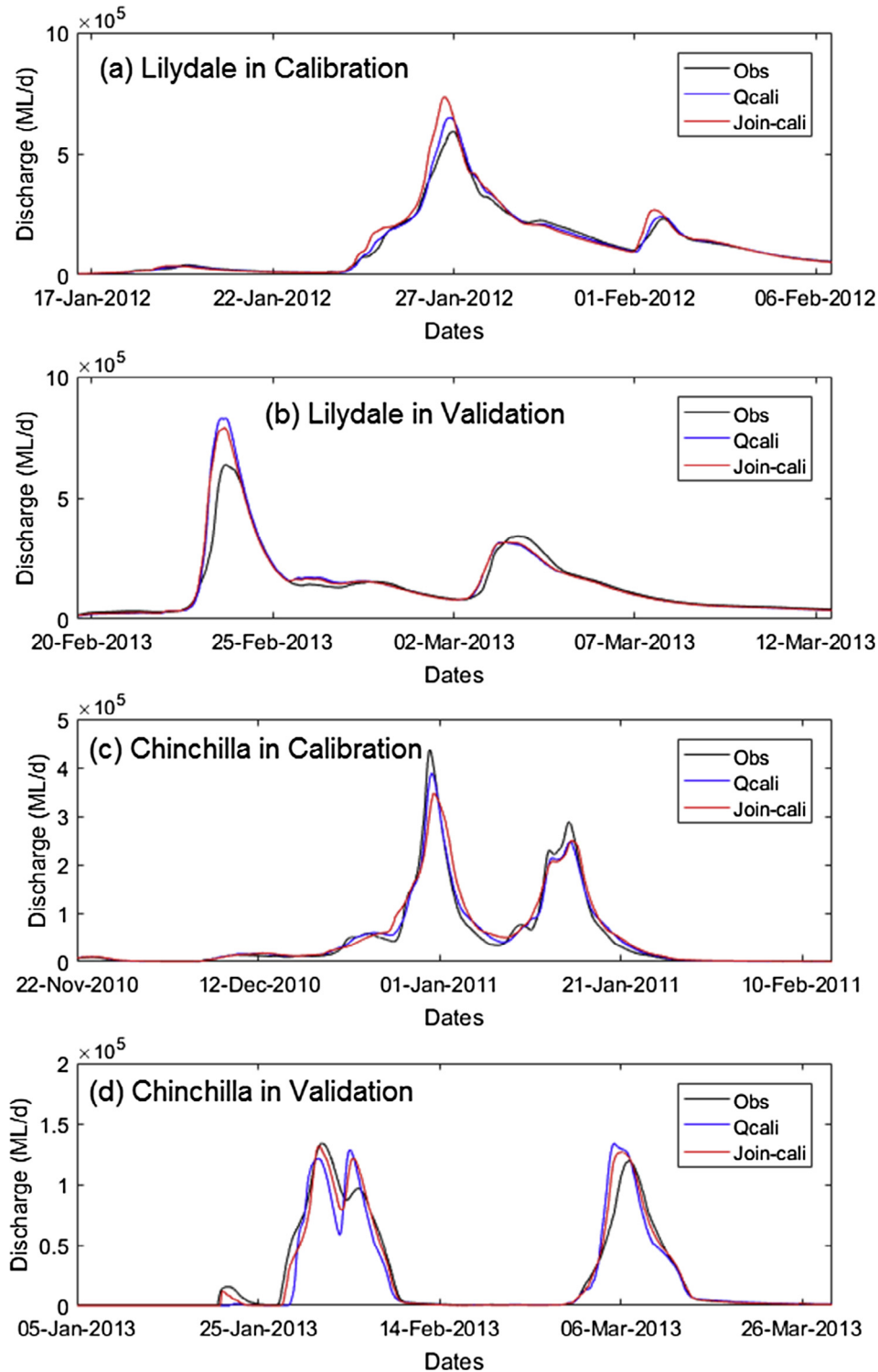


Fig. 3. Streamflow prediction at Lilydale and Chinchilla showing one flood event in the calibration period and another one in the validation period.

calibration and validation periods. Nevertheless, whether the predictions were improved or not, the difference (impact of soil moisture) tended to be stronger at the upstream and tributary sub-catchments rather than at the downstream sub-catchments.

5.2. Significance of the improvement

As discussed before, including soil moisture information into model calibration reduced the possible equifinality in global optimization. This brought benefits in two aspects. Firstly, although

minimizing errors in soil moisture simulation degraded the performance in streamflow prediction, the improved robustness in the calibration was found to exhibit the potential to improve streamflow predictions during an independent validation period, implying a possibility to improve future forecasts. Secondly, remotely sensed soil moisture brought useful spatial information to reduce the equifinality issue caused by the lack of streamflow gauges, and thus led to improvements in streamflow predictions at ungauged locations. However, the improvements in the gauged and ungauged locations were not consistent in all sub-catchments

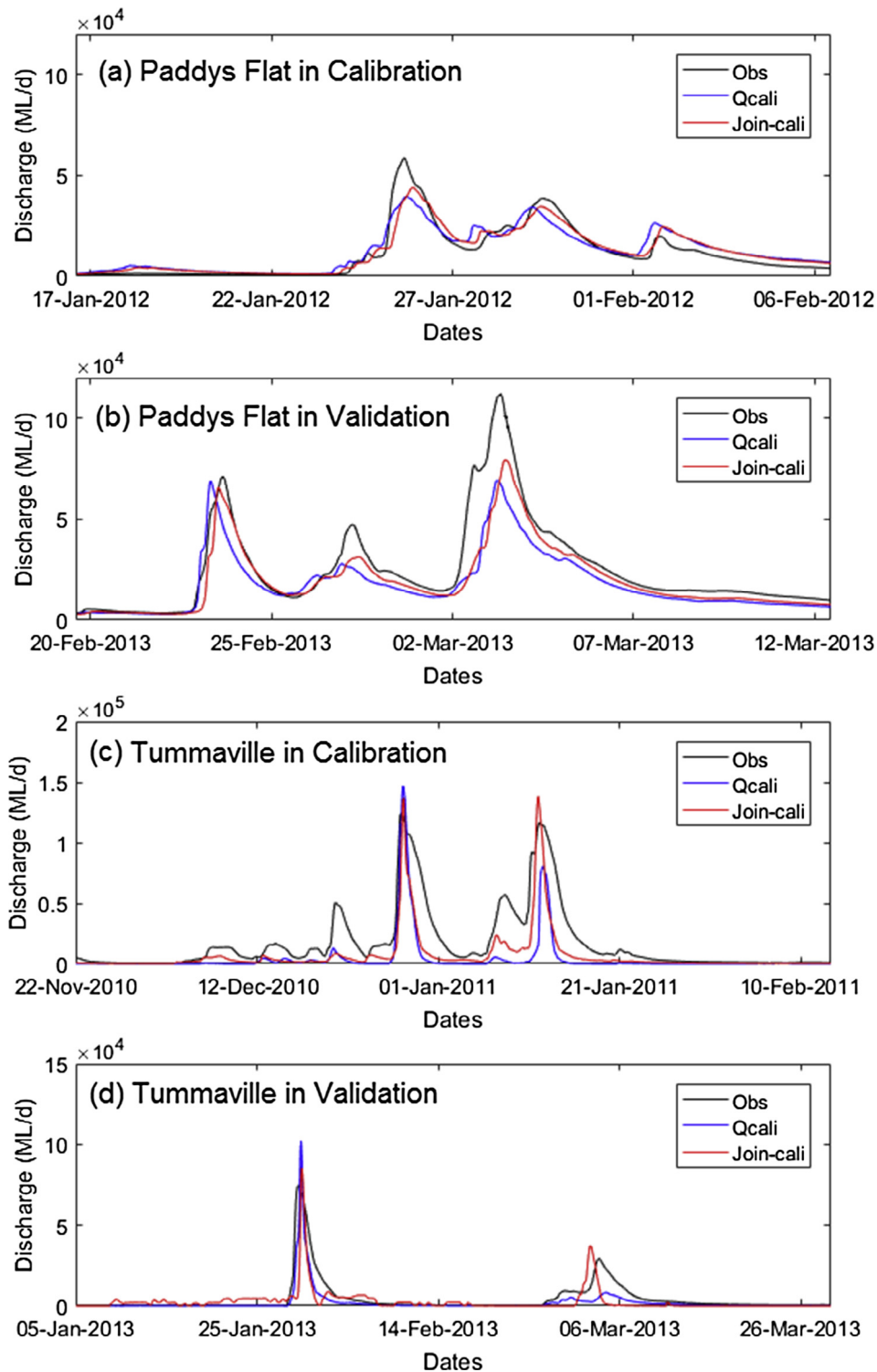


Fig. 4. Streamflow prediction at “ungauged” locations of Paddys Flat and Tummaville showing one flood event in the calibration period and another in the validation period.

according to the results shown in this study. To check the significance of such “improvements”, hypothesis student t tests were conducted for four groups of paired samples: 1) pairs of NS at “ungauged” locations from the streamflow calibration and joint calibration schemes (within the boxes in Tables 2–5); 2) pairs of F_Q at “ungauged” locations from the two calibration schemes; 3) pairs of NS at gauged locations from the two calibration schemes, but just in the independent validation period (outside the boxes in Tables 3

and 5); and 4) pairs of F_Q at gauged locations from the two calibration schemes in the independent validation period. The key procedure to conduct the hypothesis test is summarized as follows:

- Null hypothesis: the mean difference is assumed to be equal to or smaller than zero, i.e., including soil moisture for calibration does not significantly improve the performance statistics (NS or F_Q);

- Alternative hypothesis: the mean difference is greater than zero, i.e., including soil moisture for calibration significantly improves the performance statistics;
- Calculate sample differences, $d_i(NS) = NS_{i, \text{Joint-Cali}} - NS_{i, \text{Q-Cali}}$ or $d_i(F_Q) = F_{Q, i, \text{Joint-Cali}} - F_{Q, i, \text{Q-Cali}}$;
- Calculate the mean of the sample differences, \bar{d} ;
- Calculate the standard deviation of the sample differences, $\hat{\sigma} = \sqrt{\frac{1}{n} \cdot \sum_{i=1}^n (d_i - \bar{d})^2}$, where n is the sample size (15 for gauged cases and 18 for ungauged cases);
- Calculate the test statistic, $t = \frac{\bar{d} - 0}{\hat{\sigma} / \sqrt{n}}$;
- Calculate the probability (p) of the test statistic based on the student t -distribution.
- Test the null hypothesis by comparing p with target significance degree.

Fig. 5 compares the distribution of the NS and F_Q for the streamflow calibration and joint calibration schemes, while Fig. 6 shows the histograms of the sample difference distribution. It can be inferred that the improvement at “ ungauged ” locations brought by using soil moisture information is relatively more notable, while the improvement at gauged locations brought by the soil moisture in the validation period is relatively less notable.

The results from the hypothesis tests are summarized in Table 6. The p -values (probability) of the test statistics for “ ungauged ” locations were 0.0077 (<0.01) for NS and 0.0004 (<0.01) for F_Q , which indicate that the null hypothesis should be rejected in terms of both NS and F_Q ; the improvement was significant at both 0.05 and 0.01 significance degrees. The p -values for gauged locations were 0.0953 (>0.05) for NS and 0.0637 (>0.05) for F_Q , which imply that the improvement was not significant with a significance degree of 0.05.

According to the tests, it can be concluded that introducing remotely sensed soil moisture data in addition to the gauged streamflow for hydrologic model calibration brought statistically significant improvement to streamflow prediction at “ ungauged ”

locations. Whilst including soil moisture during calibration degraded the streamflow prediction at gauged locations to a slight extent, there was a possibility to improve the future forecasts at those gauged locations due to the more robust model parameter sets. However, the improvements obtained in this particular case were not statistically significant. This should be further explored in other catchments in the future.

5.3. Limitations in addressing uncertainties

The joint calibration approach proposed in this study exhibited a stronger capability to address systematic errors in parameters compared with the traditional streamflow-only calibration approach. Nevertheless, other sources of uncertainties from inputs, initial conditions and model structure were not addressed in this study. For instance, in this case study, the sub-catchment rainfall data were spatially interpolated from gauged rainfall, which is prone to instrumental and interpolation uncertainties. The uncertainty related to the interpolation process can be significant when the topography is complex and the rain gauges are sparse. Although the impact of PET was found to be much less than the rainfall (Samain and Pauwels, 2013; Bennett et al., 2014), the use of monthly interpolated gridded PET does ignore its variability within each month. The model structure and parameter uncertainties can also be considerable due to the high conceptualization in the hydrologic models, e.g., the GRKAL and linear Muskingum routing procedure used in this study. These uncertainties could potentially be further addressed through real-time updating by assimilating soil moisture and/or streamflow measurements (Wanders et al., 2014b; Alvarez-Garreton et al., 2015; Lievens et al., 2015). Therefore, it would be necessary to investigate how remotely sensed soil moisture can benefit the hydrologic prediction through an integrated calibration and real-time data assimilation system. A better estimation of the sources of uncertainties, e.g., through error decomposition approaches (Li et al., 2014; Mazrooei et al., 2015), could also be beneficial for understanding

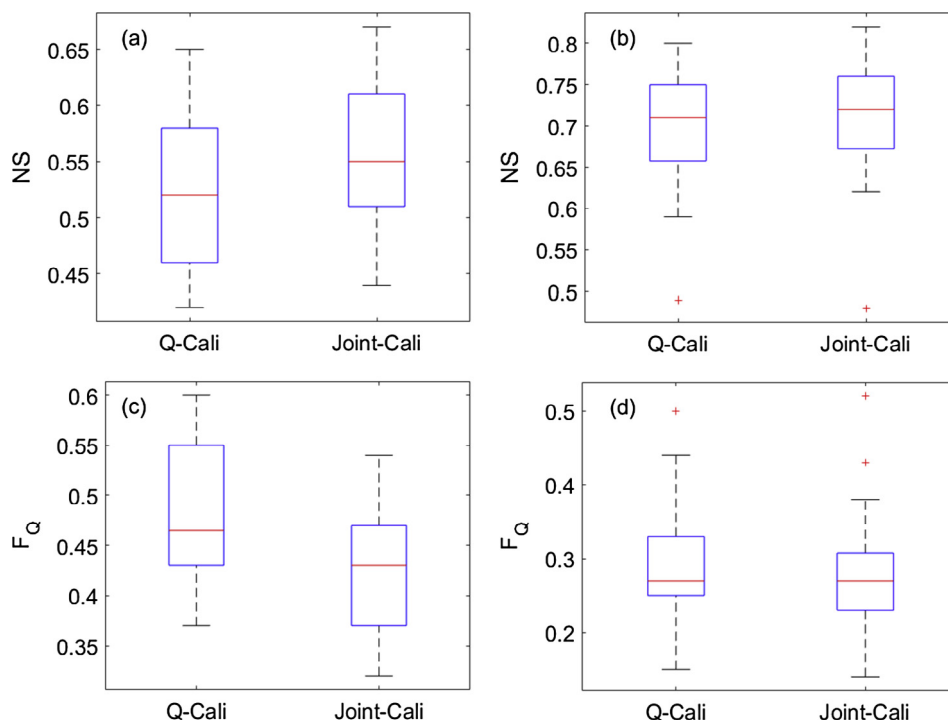


Fig. 5. Box-plots of NS and F_Q values from the streamflow calibration and joint calibration schemes. (a)/(c) illustrates the NS/ F_Q distribution at the ungauged locations; (b)/(d) illustrates the NS/ F_Q distribution at the gauged locations.

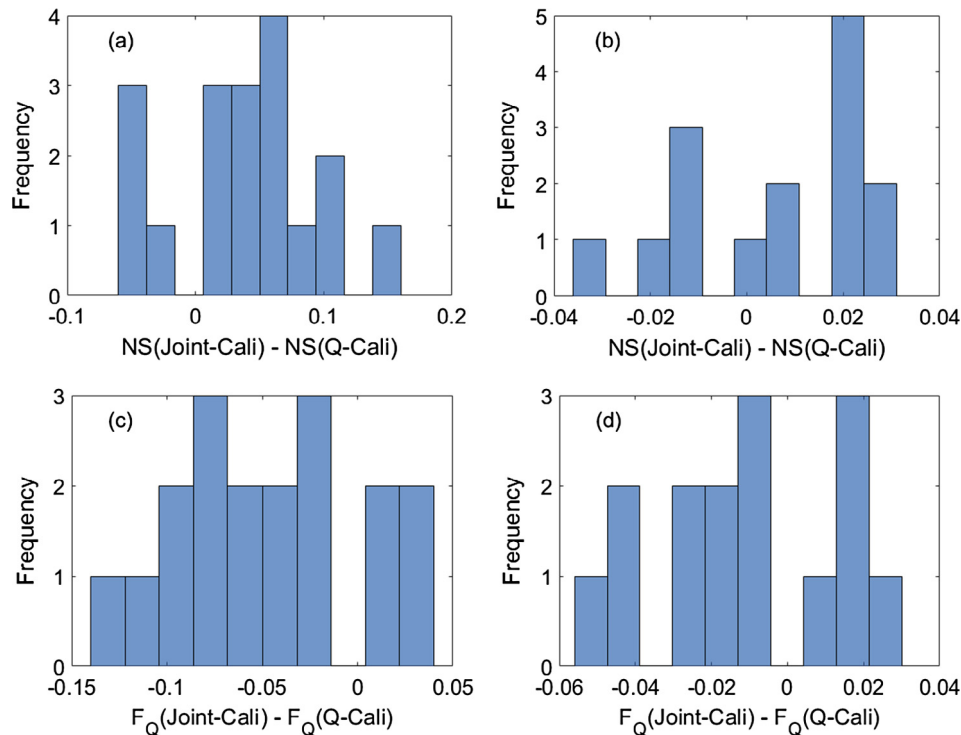


Fig. 6. Histograms of the sample differences in NS and F_Q from the streamflow calibration and joint calibration schemes. (a)/(c) illustrates the histogram of differences in NS/ F_Q at the ungauged locations; (b)/(d) illustrates the histogram of differences in NS/ F_Q at the gauged locations.

Table 6

Significance test (student t) of improvement in NS/ F_Q .

	n	Z	p
Ungauged in all periods	18	2.6913/−4.0326	0.0077/0.0004
Gauged in the validation period	15	1.3755/−1.621	0.0953/0.0637

the potential of various uncertainty reduction approaches, e.g., batch calibration and data assimilation.

In operational forecasting, forecasted rainfall and PET need to be used to force the model, which can bring additional uncertainties and affect the performance of the joint calibration approach examined in this study. Therefore, it is necessary to extend this study to operational streamflow forecasting scenarios with the consideration of forecasted forcing uncertainties.

6. Conclusions

This paper presented a joint calibration scheme using gauged streamflow and SMOS near-surface soil moisture. The joint calibration scheme was compared with a traditional streamflow only calibration scheme in three model setups, i.e., a lumped model, a semi-distributed model with only the gauge at the outlet available, and a semi-distributed model with multiple gauges available.

It was found that semi-distributed models are more suitable than lumped models in representing forcing and parameter spatial variability so as to produce more accurate streamflow predictions at the catchment outlets. The increase of the streamflow gauge availability to a large extent improved the performance of the semi-distributed model regardless of using soil moisture data for calibration. However, the impact of the soil moisture varied among different model setups.

A slight degradation in streamflow simulation was generally found at the calibration locations during the calibration period

when soil moisture was used for calibration, which is expected. However, improvements were also obtained in the independent validation period for some sub-catchments, e.g., 9 out of 15 gauged cases were improved while 5 cases were degraded slightly in terms of the NS. Although the improvement did not pass the overall significance test, it unveiled a potential to improve future forecasts through the identification of more robust parameter sets by including soil moisture information in the calibration. Future work can be dedicated to employ multiple sources of remotely sensed soil moisture data to further address this issue.

A more consistent improvement, brought by using soil moisture data, was identified at “ungauged” sub-catchments. This finding was consistent with some previous studies in which data assimilation approaches was applied, e.g., Wanders et al. (2014a) found that internal locations were improved by integrating soil moisture into a process-based model using the ensemble Kalman filter. However, there has not been a study before to investigate the potential to improve ungauged internal locations when batch calibration is used. It should also be noted that the physical linkage between soil moisture and streamflow is typically strong in process-based models and it make sense to detect improvements in streamflow estimation when soil moisture simulation is improved in those models. It is encouraging to find similar improvements at “ungauged” locations through batch calibration in a conceptual hydrologic model, and the improvement passed the statistical significance test. Furthermore, it was also found that the improvement was stronger at upstream and tributary sub-catchments than the downstream locations. The usefulness of soil moisture data for model calibration needs to be investigated under operational forecasting scenarios in future work. It would also be beneficial to use soil moisture for both batch calibration and data assimilation in an integrated system to maximize the value brought by soil moisture information.

Acknowledgements

This study was financially supported by the Bushfires & Natural Hazards CRC project - Improving flood forecast skill using remote sensing data. Valentijn Pauwels is funded by the ARC Future Fellow grant FT130100545. The authors would like to acknowledge the Australian Bureau of Meteorology and the Geoscience Australia for the valuable comments and support. The SMOS data were obtained from the “Centre Aval de Traitement des Données SMOS” (CATDS), operated for the “Centre National d’Etudes Spatiales” (CNES, France) by IFREMER (Brest, France). The MODIS vegetation cover data were obtained from the National Computational Infrastructure (NCI). The precipitation data were obtained from the Australian Bureau of Meteorology. The PET data were obtained from the Australian Water Availability Project (AWAP). The streamflow data were obtained from the New South Wales Department of Primary Industries Water and the Queensland Department of Natural Resources and Mines. All data can be provided with proper permission from the original data providers.

References

- Alvarez-Garreton, C., Ryu, D., Western, A.W., Crow, W.T., Robertson, D.E., 2014. The impacts of assimilating satellite soil moisture into a rainfall-runoff model in a semi-arid catchment. *J. Hydrol.*, 519, Part D(0):2763–2774.
- Alvarez-Garreton, C., Ryu, D., Western, A.W., Su, C.H., Crow, W.T., Robertson, D.E., Leahy, C., 2015. Improving operational flood ensemble prediction by the assimilation of satellite soil moisture: comparison between lumped and semi-distributed schemes. *Hydrol. Earth Syst. Sc.* 19 (4), 1659–1676.
- Aubert, D., Loumagne, C., Oudin, L., Le Hegarat-Masclé, S., 2003. Assimilation of soil moisture into hydrological models: the sequential method. *Canadian J. Remote Sens.* 29 (6), 711–717.
- Bennett, J.C., Robertson, D.E., Shrestha, D.L., Wang, Q.J., Enever, D., Hapuarachchi, P., Tuteja, N.K., 2014. A system for continuous hydrological ensemble forecasting (SCHEF) to lead times of 9 days. *J. Hydrol.*, 519, Part D(0):2832–2846.
- Bennett, J.C., Robertson, D.E., Ward, P.G.D., Hapuarachchi, H.A.P., Wang, Q.J., 2016. Calibrating hourly rainfall-runoff models with daily forcings for streamflow forecasting applications in meso-scale catchments. *Environ. Modelling Software* 76, 20–36.
- Brocca, L., Melone, F., Moramarco, T., Wagner, W., Naeimi, V., Bartalis, Z., Hasenauer, S., 2010. Improving runoff prediction through the assimilation of the ASCAT soil moisture product. *Hydrol. Earth Syst. Sc.* 14 (10), 1881–1893.
- Brocca, L., Moramarco, T., Melone, F., Wagner, W., Hasenauer, S., Hahn, S., 2012. Assimilation of surface- and root-zone ASCAT soil moisture products into rainfall-runoff modelling. *IEEE Trans. Geosci. Remote Sens.* 50 (7), 2542–2555.
- Cenci, L., Laiolo, P., Gabellani, S., Campo, L., Silvestro, F., Delogu, F., Boni, G., Rudari, R., 2016. Assimilation of H-SAF soil moisture products for flash flood early warning systems. Case study: Mediterranean catchments. *IEEE J. Selected Top. Appl. Earth Observations Remote Sens.* 9 (12), 5634–5646.
- Chen, F., Crow, W.T., Ryu, D., 2014. Dual forcing and state correction via soil moisture assimilation for improved rainfall-runoff modelling. *J. Hydrometeorol.* 15 (5), 1832–1848.
- Chen, F., Crow, W.T., Starks, P.J., Moriasi, D.N., 2011. Improving hydrologic predictions of a catchment model via assimilation of surface soil moisture. *Adv. Water Resour.* 34 (4), 526–536.
- Crow, W.T., Ryu, D., 2009. A new data assimilation approach for improving runoff prediction using remotely-sensed soil moisture retrievals. *Hydrol. Earth Syst. Sc.* 13 (1), 1–16.
- Cunge, J.A., 1969. On the subject of a flood propagation computation method (Muskingum Method). *J. Hydraul. Res.* 7 (2), 205–230.
- Draper, C.S., Mahfouf, J.F., Calvet, J.C., Martin, E., Wagner, W., 2011. Assimilation of ASCAT near-surface soil moisture into the SIM hydrological model over France. *Hydrol. Earth Syst. Sc.* 15 (12), 3829–3841.
- Duan, Q., Sorooshian, S., Gupta, H.V., 1992. Effective and efficient global optimization for conceptual rainfall-runoff models. *Water Resour. Res.* 28 (4), 1015–1031.
- Emerton, R.E., Stephens, E.M., Pappenberger, F., Pagano, T.C., Weerts, A.H., Wood, A.W., Salamon, P., Brown, J.D., Hjerdt, N., Donnelly, C., Baugh, C.A., Cloke, H.L., 2016. Continental and global scale flood forecasting systems. *Wiley Interdisciplinary Rev. Water* 3, 391–418.
- Francois, C., Quesney, A., Ottlé, C., 2003. Sequential assimilation of ERS-1 SAR data into a coupled land surface-hydrological model using an extended Kalman filter. *J. Hydrometeorol.* 4 (2), 473–487.
- Goodrich, D.C., Schmugge, T.J., Jackson, T.J., Unkrich, C.L., Keefer, T.O., Parry, R., Bach, L.B., Amer, S.A., 1994. Runoff simulation sensitivity to remotely sensed initial soil water content. *Water Resour. Res.* 30 (5), 1393–1405.
- Grimaldi, S., Li, Y., Pauwels, V.R.N., Walker, J.P., 2016. Remote sensing-derived water extent and level to constrain hydraulic flood forecasting models: opportunities and challenges. *Surv. Geophys.* 37 (5), 977–1034.
- Han, E., Merwade, V., Heathman, G.C., 2012. Implementation of surface soil moisture data assimilation with watershed scale distributed hydrological model. *J. Hydrol.* 416–417, 98–117.
- Haynes, K., Coates, L., de Oliveira, F., Gissing, A., Bird, D., van den Honert, R.R., D’Arcy, R., Smith, C., 2016. An analysis of human fatalities from floods in Australia 1900–2015. 166, *Bushfire and Natural Hazards CRC*.
- Jacobs, J.M., Myers, D.A., Whitfield, B.M., 2003. Improved rainfall/runoff estimates using remotely sensed soil moisture. *J. Am. Water Resour. Assoc.* 39 (2), 313–324.
- Kundu, D., Vervoort, R.W., van Ogtrop, F.F., 2017. The value of remotely sensed surface soil moisture for model calibration using SWAT. *Hydrol. Process.* 31 (15), 2764–2780.
- Kunnath-Poovakka, A., Ryu, D., Renzullo, L.J., George, B., 2016. The efficacy of calibrating hydrologic model using remotely sensed evapotranspiration and soil moisture for streamflow prediction. *J. Hydrol.* 535, 509–524.
- Laiolo, P., Gabellani, S., Campo, L., Cenci, L., Silvestro, F., Delogu, F., Boni, G., Rudari, R., Puca, S., Pisani, A.R., 2015. Assimilation of remote sensing observations into a continuous distributed hydrological model: impacts on the hydrologic cycle, 2015 IEEE International Geoscience and Remote Sensing Symposium (IGARSS), pp. 1308–1311.
- Legates, D.R., Mahmood, R., Levina, D.F., DeLiberty, T.L., Quiring, S.M., Houser, C., Nelson, F.E., 2011. Soil moisture: a central and unifying theme in physical geography. *Prog. Phys. Geogr.* 35 (1), 65–86.
- Li, Y., Grimaldi, S., Walker, J., Pauwels, V., 2016. Application of remote sensing data to constrain operational rainfall-driven flood forecasting: a review. *Remote Sens.* 8 (6), 456.
- Li, Y., Ryu, D., Western, A.W., Wang, Q.J., 2013. Assimilation of stream discharge for flood forecasting: the benefits of accounting for routing time lags. *Water Resour. Res.* 49 (4), 1887–1900.
- Li, Y., Ryu, D., Western, A.W., Wang, Q.J., 2015. Assimilation of stream discharge for flood forecasting: Updating a semidistributed model with an integrated data assimilation scheme. *Water Resour. Res.* 51 (5), 3238–3258.
- Li, Y., Ryu, D., Western, A.W., Wang, Q.J., Robertson, D.E., Crow, W.T., 2014. An integrated error parameter estimation and lag-aware data assimilation scheme for real-time flood forecasting. *J. Hydrol.*, 519, Part D(0): 2722–2736.
- Lievens, H., Tomer, S.K., Al Bitar, A., De Lannoy, G.J.M., Drusch, M., Dumedah, G., Hendricks Franssen, H.J., Kerr, Y.H., Martens, B., Pan, M., Roundy, J.K., Vereecken, H., Walker, J.P., Wood, E.F., Verhoest, N.E.C., Pauwels, V.R.N., 2015. SMOS soil moisture assimilation for improved hydrologic simulation in the Murray Darling Basin, Australia. *Remote Sens. Environ.* 168, 146–162.
- Liu, Y., Weerts, A.H., Clark, M., Hendricks Franssen, H.J., Kumar, S.V., Moradkhani, H., Seo, D.J., Schwanenber, D., Smith, P., van Dijk, A.I.J.M., van Velzen, N., He, M., Lee, H., Noh, S.J., Rakovec, O., Restrepo, P., 2012. Advancing data assimilation in operational hydrologic forecasting: progresses, challenges, and emerging opportunities. *Hydrol. Earth Syst. Sc.* 16 (10), 3863–3887.
- López López, P., Sutanudjaja, E.H., Schellekens, J., Sterk, G., Bierkens, M.F.P., 2017. Calibration of a large-scale hydrological model using satellite-based soil moisture and evapotranspiration products. *Hydrol. Earth Syst. Sci.* 21 (6), 3125–3144.
- López López, P., Wanders, N., Schellekens, J., Renzullo, L.J., Sutanudjaja, E.H., Bierkens, M.F.P., 2016. Improved large-scale hydrological modelling through the assimilation of streamflow and downscaled satellite soil moisture observations. *Hydrol. Earth Syst. Sc.* 20 (7), 3059–3076.
- Loumagne, C., Chkir, N., Normand, M., Ottlé, C., Vidal-Madjar, D., 1996. Introduction of the soil/vegetation/atmosphere continuum in a conceptual rainfall/runoff model. *Hydrol. Sci. J.* 41 (6), 889–902.
- Loumagne, C., Normand, M., Riffard, M., Weisse, A., Quesney, A., HEGarat-Masclé, S. L., Alem, F., 2001a. Integration of remote sensing data into hydrological models for reservoir management. *Hydrol. Sci. J.* 46 (1), 89–102.
- Loumagne, C., Weisse, A., Normand, M., Riffard, M., 2001b. Integration of remote sensing data into hydrological models for flood forecasting. *Remote Sensing and Hydrology 2000*. I.A.H.S. Publication, Santa Fe, New Mexico, USA, pp. 592–594.
- Massari, C., Brocca, L., Barbetta, S., Papathanasiou, C., Mimikou, M., Moramarco, T., 2014. Using globally available soil moisture indicators for flood modelling in Mediterranean catchments. *Hydrol. Earth Syst. Sc.* 18 (2), 839–853.
- Matgen, P., Fenicia, F., Heitz, S., Plaza, D., de Keyser, R., Pauwels, V.R.N., Wagner, W., Savenije, H., 2012. Can ASCAT-derived soil wetness indices reduce predictive uncertainty in well-gauged areas? A comparison with in situ observed soil moisture in an assimilation application. *Adv. Water Resour.* 44, 49–65.
- Mazrooei, A., Sinha, T., Sankarasubramanian, A., Kumar, S., Peters-Lidard, C.D., 2015. Decomposition of sources of errors in seasonal streamflow forecasting over the U.S. Sunbelt. *J. Geophys. Res. Atmos.* 120 (23), 11809–11825.
- Nash, J.E., 1959. A Note on the Muskingum Flood-Routing Method. *J. Geophys. Res.* 64 (8), 1053–1056.
- Ottlé, C., Vidal-Madjar, D., 1994. Assimilation of soil moisture inferred from infrared remote sensing in a hydrological model over the HAPEX-MOBILHY region. *J. Hydrol.* 158 (3–4), 241–264.
- Pagano, T.C., Pappenberger, F., Wood, A.W., Ramos, M.-H., Persson, A., Anderson, B., 2016. Automation and human expertise in operational river forecasting. *Wiley Interdisciplinary Rev. Water: n/a-n/a*.
- Pagano, T.C., Wang, Q.J., Hapuarachchi, P., Robertson, D., 2011a. A dual-pass error-correction technique for forecasting streamflow. *J. Hydrol.* 405 (3–4), 367–381.
- Pagano, T.C., Ward, P., Wang, X.N., Hapuarachchi, P., Shrestha, D.L., Anticev, J., Wang, Q.J., 2011b. The SWIFT calibration cookbook: experience from the Ovens. *CSIRO, Water for a Healthy Country National Research Flagship*.

- Pagano, T.C., Wood, A.W., Ramos, M.-H., Cloke, H.L., Pappenberger, F., Clark, M.P., Cranston, M., Kavetski, D., Mathevet, T., Sorooshian, S., Verkade, J.S., 2014. Challenges of operational river forecasting. *J. Hydrometeorol.* 15, 1692–1707.
- Parajka, J., Naeimi, V., Blöschl, G., Komma, J., 2009. Matching ERS scatterometer based soil moisture patterns with simulations of a conceptual dual layer hydrologic model over Austria. *Hydrol. Earth Syst. Sc.* 13 (2), 259–271.
- Parajka, J., Naeimi, V., Blöschl, G., Wagner, W., Merz, R., Scipal, K., 2006. Assimilating scatterometer soil moisture data into conceptual hydrologic models at the regional scale. *Hydrol. Earth Syst. Sc.* 10 (3), 353–368.
- Pauwels, V.R.N., Hoeben, R., Verhoest, N.E.C., De Troch, F.P., 2001. The importance of the spatial patterns of remotely sensed soil moisture in the improvement of discharge predictions for small-scale basins through data assimilation. *J. Hydrol.* 251 (1–2), 88–102.
- Pauwels, V.R.N., Hoeben, R., Verhoest, N.E.C., De Troch, F.P., Troch, P.A., 2002. Improvement of TOPLATS-based discharge predictions through assimilation of ERS-based remotely sensed soil moisture values. *Hydrol. Process.* 16 (5), 995–1013.
- Priestley, C.H.B., Taylor, R.J., 1972. On the assessment of surface heat flux and evaporation using large-scale parameters. *Mon. Weather Rev.* 100 (2), 81–92.
- Quesney, A., Francois, C., Ottlé, C., Le Hegarat, S., Loumagne, C., Normand, M., 2001. Sequential assimilation of SAR/ERS data in a lumped rainfall-runoff model with an extended Kalman filter. In: Owe, M., Braubaker, K., Ritchie, J., Rango, A. (Eds.), *Remote Sensing and Hydrology 2000*. Iahs Publication, pp. 495–497.
- Rajib, M.A., Merwade, V., Yu, Z., 2016. Multi-objective calibration of a hydrologic model using spatially distributed remotely sensed/in-situ soil moisture. *J. Hydrol.* 536, 192–207.
- Raupach, M.R., Briggs, P.R., Haverd, V., King, E.A., Paget, M., Trudinger, C.M., 2009. Australian Water Availability Project (AWAP): CSIRO Marine and Atmospheric Research Component: Final Report for Phase 3, CSIRO Marine and Atmospheric Research, Aspendale.
- Raupach, M.R., Briggs, P.R., Haverd, V., King, E.A., Paget, M., Trudinger, C.M., 2012. Australian Water Availability Project. CSIRO Marine and Atmospheric Research, Canberra, Australia.
- Ridler, M.-E., Madsen, H., Stisen, S., Bircher, S., Fensholt, R., 2014. Assimilation of SMOS-derived soil moisture in a fully integrated hydrological and soil-vegetation-atmosphere transfer model in Western Denmark. *Water Resour. Res.* 50 (11), 8962–8981.
- Robertson, D.E., Bennett, J.C., Wang, Q.J., 2015. A strategy for quality controlling hourly rainfall observations and its impact on hourly streamflow simulations. In: Weber, T., McPhee, M.J., Anderssen, R.S. (Eds.), *MODSIM2015, 21st International Congress on Modelling and Simulation*. Modelling and Simulation Society of Australia and New Zealand, Gold Coast, Australia, pp. 2110–2116.
- Romano, N., 2014. Soil moisture at local scale: measurements and simulations. *J. Hydrol.* 516, 6–20.
- Samain, B., Pauwels, V.R.N., 2013. Impact of potential and (scintillometer-based) actual evapotranspiration estimates on the performance of a lumped rainfall-runoff model. *Hydrol. Earth Syst. Sci.* 17 (11), 4525–4540.
- Sene, K., 2008. *Flood Warning. Forecasting and Emergency Response*, Springer, Berlin, London.
- Shahrban, M., 2017. *On the Importance of Soil Moisture for Streamflow Forecasting*. Monash University.
- Silvestro, F., Gabellani, S., Rudari, R., Delogu, F., Laiolo, P., Boni, G., 2015. Uncertainty reduction and parameter estimation of a distributed hydrological model with ground and remote-sensing data. *Hydrol. Earth Syst. Sc.* 19 (4), 1727–1751.
- Sutanudjaja, E.H., van Beek, L.P.H., de Jong, S.M., van Geer, F.C., Bierkens, M.F.P., 2014. Calibrating a large-extent high-resolution coupled groundwater-land surface model using soil moisture and discharge data. *Water Resour. Res.* 50 (1), 687–705.
- Thorstensen, A., Nguyen, P., Hsu, K., Sorooshian, S., 2016. Using densely distributed soil moisture observations for calibration of a hydrologic model. *J. Hydrometeorol.* 17 (2), 571–590.
- Wanders, N., Bierkens, M.F.P., de Jong, S.M., de Roo, A., Karssenberg, D., 2014a. The benefits of using remotely sensed soil moisture in parameter identification of large-scale hydrological models. *Water Resour. Res.* 50 (8), 6874–6891.
- Wanders, N., Karssenberg, D., de Roo, A., de Jong, S.M., Bierkens, M.F.P., 2014b. The suitability of remotely sensed soil moisture for improving operational flood forecasting. *Hydrol. Earth Syst. Sc.* 18 (6), 2343–2357.
- Yan, H., Moradkhani, H., 2016. Combined assimilation of streamflow and satellite soil moisture with the particle filter and geostatistical modelling. *Adv. Water Resour.* 94, 364–378.
- Zhang, Y., Li, Y., Walker, J.P., Pauwels, V.R.N., Shahrban, M., 2015. Towards operational hydrological model calibration using streamflow and soil moisture measurements, 21st International Congress on Modelling and Simulation. Gold Coast, Australia, pp. 2089–2095.